ELSEVIER

Physica B 300 (2001) 78–90

PHYSICA B

www.elsevier.com/locate/physb

Erbium as a probe of everything?

A. Polman*

FOM-Institute for Atomic and Molecular Physics (AMOLF), Kruislaan 407, 1098 SJ Amsterdam, The Netherlands

Received 20 April 2001; accepted 11 May 2001

Abstract

Erbium is a lanthanide ion with unique electronic and optical properties. In its trivalent state it is composed of an incompletely filled 4f inner shell and two closed outer shells. By employing these properties in specific material systems, Er can be used to probe point defects, oxygen, OH, Er, radiation defects, network structure, excitons, optical density of states, optical modes, and photonic bandstructure. © 2001 Elsevier Science B.V. All rights reserved.

Keywords: Erbium

1. Introduction

Erbium (^{68}Er) is the 11th ion in the lanthanide series ^{58}Ce–^{71}Lu. Erbium as an element was first discovered and identified in the Swedish town of Ytterby in 1842. Its electronic structure is [Xe] $4f^{12}$ $6s^2$. Pure erbium is a metal. When incorporated as an impurity into a dielectric host, Er usually takes the trivalent charge state with electronic configuration: [Xe] $4f^{11}$. This configuration is special, as it is composed of an incompletely filled 4f shell that is shielded from the surrounding matrix by two closed 5s and 5p shells. The 4f electrons interact by spin–spin and spin–orbit interaction. The two interactions are of similar strength and lead to relatively large differences between the 4f energy levels. Fig. 1 shows a schematic of the 4f energy levels of Er, both for a free ion, and in a solid host where Stark splitting occurs as the degenerate 4f levels split up in the electric field caused by the local atomic configuration around the Er^{3+} ion. Due to the shielding effect of the outer shells, the exact energies of the 4f states differ only slightly for different hosts in which Er is incorporated. Erbium has become a technologically important ion as the transition from the first excited state to the ground state ($\Delta E = 6500\,cm^{-1}$, corresponding to $\lambda = 1.54\,\mu m$), incidentally coincides with the wavelength of maximum transmission in silica optical fiber that is used in optical telecommunication technology. The revolution in communication technology that is presently taking place can be entirely attributed to the fact that erbium-doped optical fiber amplifiers have been developed that have made long-distance optical communication possible.

Due to its unique electronic properties, erbium is an interesting probe for a large variety of physical effects. As we will show in this article, the specific properties of the outer (binding) electrons make Er a sensitive probe for structural defects (e.g. point defects), impurities (e.g. oxygen), and excitons in semiconductors. As the other lanthanide ions in the series have similar outer shell configurations, these probing effects are to some

*Tel.: + 31-20-608-1234; fax: + 31-20-668-4106.
E-mail address: polman@amolf.nl (A. Polman).

0921-4526/01/$ - see front matter © 2001 Elsevier Science B.V. All rights reserved.
PII: S 0 9 2 1 - 4 5 2 6 (0 1) 0 0 5 7 3 - 7

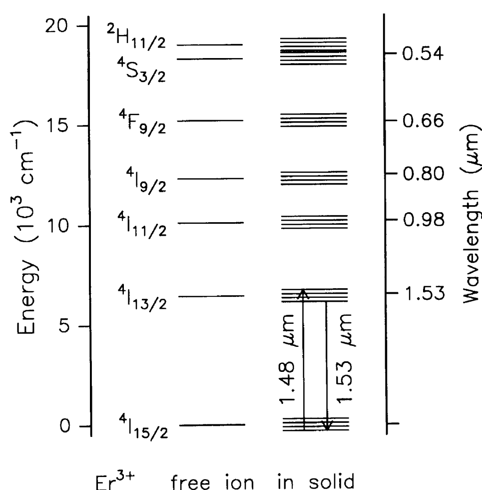

Fig. 1. Energy levels of Er^{3+}. Data are shown both for the Er^{3+} free ion, and for Er in a solid host.

extent universal for the lanthanide ions. X-ray absorption spectroscopy on the Er L_{III} inner shell can be used to probe the glass network configuration around Er ions. The 4f shell properties of Er can be exploited to probe a variety of optical effects. By studying non-radiative processes, the coupling of Er to vibrational states of impurities such as OH can be studied. Studies of non-radiative processes can also be used to probe irradiation defects that are present in glass. Interactions among Er ions can be probed by studying Förster energy transfer [1,2] between excited ions. Optical modes and the local optical density of states in thin-film dielectric photonic materials and photonic crystals can be probed by Er with great accuracy. In this paper, 10 different examples of these probing effects of Er are presented that have been studied in our group. Each description is relatively brief, and reference is made to work in which each of the effects is described in more detail.

2. Erbium as a probe of point defects

Amorphous silicon (a-Si) is an important material that finds applications in for example thin-film transistors or solar cells. In its most pure form, a-Si has a continuous random network structure in which each Si atom is coordinated with on average four Si atoms. Due to the amorphous nature of the network, the actual coordination as well as the Si–Si bond angles vary over a continuous range throughout the material. In the past, significant effort has been put in identifying the structure of a-Si. [3] One question that was posed is whether point defects exist in the a-Si network structure.

Erbium can be used as a probe of point defects, by studying its diffusion and segregation at a moving interface between single-crystal and amorphous Si. To study this, 250 keV Er ions were implanted in single crystal Si at fluences in the range $(0.6–9.0) \times 10^{14}$ cm^{-2}, large enough to cause full amorphization of the crystalline surface layer. The peak Er concentration in the a-Si layer was in the range 10^{19}–10^{20} cm^{-3}, depending on the fluence. Upon annealing at a temperature of 600°C, the amorphous layer recrystallizes by solid-phase epitaxial growth [4]. As erbium is nearly completely insoluble in crystalline Si (by analogy with the transition elements the solubility is estimated to be 10^{14}–10^{16} cm^{-3}), Er at the moving interface will segregate into the amorphous layer, in order to escape from the growing crystal. High-resolution Rutherford backscattering spectrometry (RBS) was used to determine the Er depth profile around the interface [5]. Two characteristic profiles for two different Er fluences are shown in Fig. 2. For the low fluence case, a Gaussian-shaped peak is found around the interface, corresponding to a narrow segregation spike with a deconvoluted width $\sigma = 0.9$ nm. For the higher Er fluence a flat-topped profile, located on the amorphous side of the interface is observed. These data are consistent with the idea of segregation and trapping at point defects in a-Si, as described in detail in Ref. [5]. For low Er fluence, all Er is segregated from the growing crystal and trapped at point defects on the a-Si side of the interface (see lower inset in Fig. 2). For higher Er fluences, once a significant segregation spike has built up at the interface, all point defects in a-Si near the interface are occupied. As a result trapping will also occur on the crystalline side of the interface, as observed in Fig. 2. In addition, rapid diffusion of Er in excess of the trap density will occur, leading to the flat-topped Er profile on

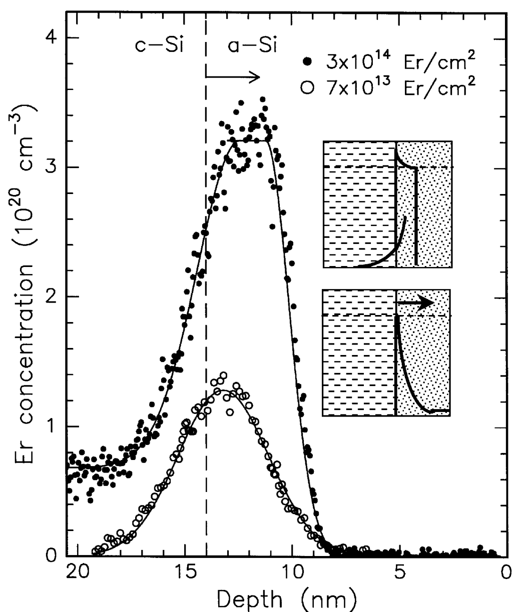

Fig. 2. Erbium as a probe of point defects. Erbium concentration depth profiles around a crystal–amorphous Si interface during solid-phase epitaxial growth. Data were taken using high-resolution RBS using a 100 keV H^+ beam in combination with an electrostatic analyzer. From Polman et al. [5]. The schematic insets show how the segregation occurs for Er concentrations below and above the defect level. From the data the defect density in amorphous Si was estimated.

the a-Si side (see upper inset in Fig. 2). From these segregation and trapping experiments, the defect trap density in a-Si annealed at 600°C was estimated to be 0.6 at% [5]. Experiments on the segregation and trapping of praseodymium [6], another lanthanide ion, showed similar results as those for Er, consistent with the notion that these phenomena are due to the outer-shell electronic configuration.

3. Erbium as a probe of O

Erbium in silicon reacts strongly with oxygen. This effect was first noticed when the optical properties of Er-doped Si were studied for Si doped with high and low O content [7–9]. In both the cases, 1.5 μm photoluminescence was observed at low temperature (15 K). However, without O strong temperature quenching of the luminescence was observed, while in highly O doped Si (10^{18}–10^{20} cm^{-3}) this effect was strongly reduced. The strong effect of O was attributed to the formation of Er–O complexes, as was confirmed by X-ray absorption fine structure spectroscopy (EXAFS) [10].

We [6], and others [11], have studied the reaction between Er and O using segregation studies. Er was implanted into a single-crystal Si wafer of which a 780 nm thick surface layer was first

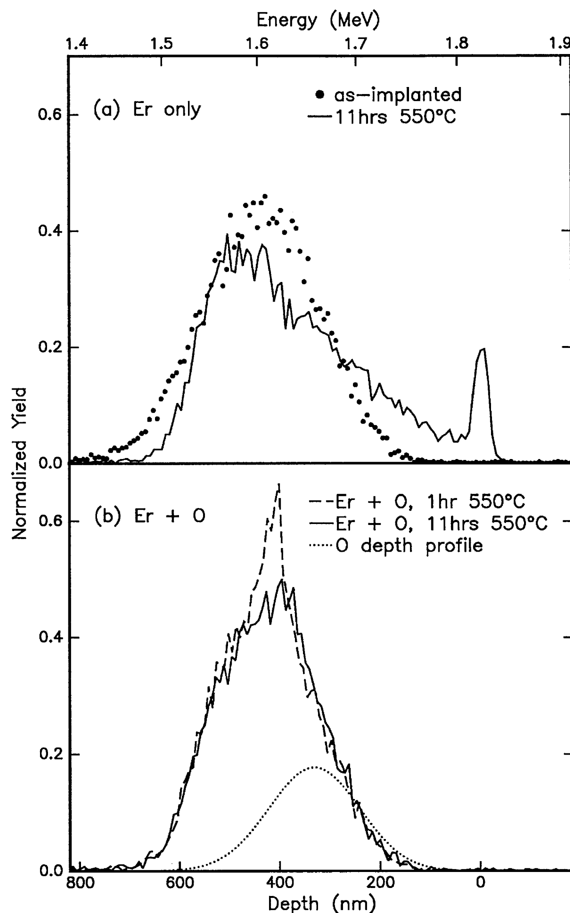

Fig. 3. Erbium as a probe of oxygen. Erbium concentration depth profiles in silicon measured using RBS with a 2 MeV He^+ beam. A 780 nm thick amorphous Si layer was implanted with 1.6×10^{15} Er cm^{-2} at 1.5 MeV and then recrystallized at 550°C. (a) as-implanted profile (dots), and profile after annealing for 11 h. (drawn line). (b) Er depth profiles after annealing in a sample co-doped with oxygen (5×10^{15} O cm^{-2}, 160 keV). The O depth profile is shown as the dotted line. From Custer et al. [6]. Oxygen strongly reduces the segregation of Er.

amorphized by Si irradiation. Upon thermal annealing at 550°C, the layer is recrystallized. Fig. 3(a) shows a depth profile measured using RBS of the as-implanted Er profile, and the profile after crystallization. A clear shift towards the surface is observed, indicative of segregation. This segregation effect is similar to that discussed in Section 2. With O co-doping, nearly no segregation is observed as can be seen in Fig. 3(b) which shows two Er profiles; one after 1 h annealing for which partial regrowth is observed, with a segregation spike visible at a depth of 400 nm, and one for full recrystallization (11 h annealing). The oxygen depth profile is shown in Fig. 3(b) by the dotted line. Its peak concentration amounts to 1.5×10^{20} O cm^{-3}. The enhanced trapping is explained in terms of the formation of Er–O complexes that would show no segregation. Alternatively, it could be that O saturates defect traps in a-Si, thereby increasing the trapping (see Section 2). We note that a similar reduction in segregation of Er during crystal growth is observed during molecular beam epitaxial growth of Er-doped Si [12]. We also studied the effect of O on the segregation of holmium, another lanthanide ion, and found the same results as for Er [13], consistent with the fact that these lanthanide–oxygen complex formation phenomena are due to the outer-shell electronic configuration.

4. Erbium as a probe of OH

Erbium-doped silica glass is being used in optical fiber amplifiers in telecommunication links to regenerate the optical signal that is gradually absorbed and scattered along the length of the fiber. More recently, Er-doped *planar* optical amplifiers have become a topic of great interest. In these amplifiers, an Er-doped waveguide is integrated on a planar substrate [14]. These devices have much smaller size than the fiber amplifiers, and therefore, are of great interest in local photonic networks in which small size is important. In addition, planar amplifiers can be integrated with other devices such as optical splitters, wavelength multiplexers, and optical switches on the same substrate.

In order to achieve optical amplification in a planar waveguide with small dimensions, high Er concentrations are required. One of the effects that limit the Er concentration that can be incorporated is a luminescence quenching effect—if the Er concentration typically exceeds 0.1 at%, the average distance between Er ions is so small that an excited Er ion can transfer its energy to a nearby unexcited ion through a Förster transfer mechanism. In this way, energy can migrate through the glass. This in itself would not have a detrimental effect on the average excited Er population, unless quenching centers are present in the glass. One impurity that is known to be a strong quencher of Er is OH, as the second overtone of the OH stretch vibration is resonant with the first excited state of Er. In highly Er doped glass, in which energy migration can take place over a significant distance, a small concentration of OH will cause significant quenching.

Fig. 4(a) shows a photoluminescence (PL) spectrum of Er-implanted sodalime silicate glass (500 keV, 3.7×10^{15} Er cm^{-2}, 0.4 at% peak) after annealing at 512°C [15]. Two main peaks are observed at 1.537 and 1.545 μm. All peaks are due to inhomogeneously broadened transitions between the Stark manifolds (see Fig. 1). Fig. 4(b) shows measurements of the PL lifetime measured at 1.537 μm [16]. The Er concentration for the highest fluence in Fig. 4(b) amounts to 1.4×10^{21} cm^{-3} (2.1 at%). As can be seen, the lifetime shows a roughly linear increase with Er concentration. This is consistent with a simple concentration quenching model, in which the Er decay rate (R_{Er}) is linearly proportional to the Er concentration and the quencher concentration: $R_{\mathrm{Er}} = C_{\mathrm{Er-Er}}[\mathrm{Er}][\mathrm{OH}]$, with $C_{\mathrm{Er-Er}}$ a coupling constant that reflects the Förster energy transfer rate between Er ions. Additional measurements, in which the Er concentration was kept fixed but the OH concentration varied further confirm this model [17]. As the coupling constants $C_{\mathrm{Er-Er}}$ are known for a variety of materials, PL lifetime measurements can be used as a fast probe of the OH content in an Er-doped film. Coupling between Er and OH has also been observed in organic cage complexes that were designed to incorporate Er in polymer waveguide films [18].

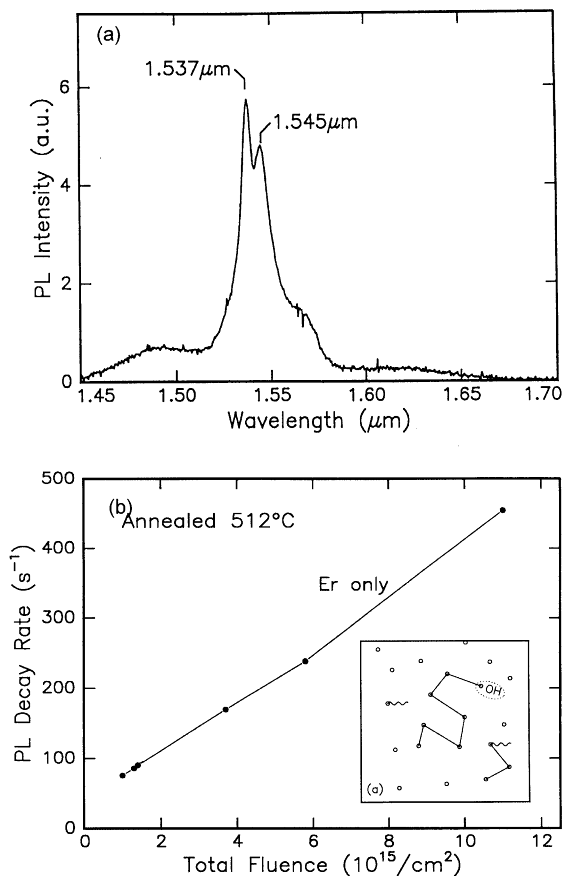

Fig. 4. Erbium as a probe of OH. (a) PL spectrum of Er-implanted sodalime silicate glass (500 keV, 3.7×10^{15} Er cm^{-2}) after annealing at 512°C (1 h.). (b) PL lifetime measurements as a function of Er implantation fluence. A schematic of the concentration quenching process is shown in the inset. From Snoeks et al. [15,16]. A high OH content causes strong quenching of the Er photoluminescence.

The Er luminescence lifetime of Er in these complexes is in the μs range. In this case, the OH quenchers originate from water in the solvents used to prepare these organic complexes.

5. Erbium as a probe of erbium

The design and fabrication of Er-doped planar amplifiers has been intensively studied over the past ten years. Initially, most research focussed on the incorporation of Er in different host materials and measurements of luminescence spectra and lifetimes. At the same time, many advances were made in waveguide fabrication technology. In more recent years, actual Er-doped waveguide amplifiers were fabricated that showed a net optical gain [14]. It was found that gain was only achieved for an Er concentration in a narrow concentration window, for waveguides with optical losses typically well below 1 dB cm^{-1}. The major gain limiting effect is a cooperative upconversion interaction in which two Er ions in the $^4I_{13/2}$ state can interact through a Förster mechanism [19,20]. As schematically indicated in Fig. 5(a), one excited ion can become de-excited by transferring its energy to a nearby excited ion, which is then promoted to the $^4I_{9/2}$ level. From there it will rapidly relax to the $^4I_{11/2}$ level. A second-order upconversion process, in which Er ions in the $^4I_{11/2}$ state interact will promote one ion to the $^4H_{11/2}$ state. These upconversion interactions can be very strong at the high concentrations (0.1–1.0 at%) required to achieve high gain per unit length, and are detrimental for the optical gain. Upconversion increases the pump power to reach a certain degree of inversion. This in itself can be detrimental because at high pump power, excited state absorption will occur, in which a pump photon is absorbed by Er in the $^4I_{13/2}$ state, thereby bringing it into an (undesired) higher state.

Fabrication of an optimized optical waveguide material requires minimizing of upconversion interactions, and therefore achieving a homogeneous Er distribution at the atomic scale. To illustrate this, Figs. 5(b) and (c) show optical images of the green second-order upconversion emission from two different Er-doped planar Al_2O_3 waveguide spirals doped to a concentration of 0.2 at%, both pumped at 1.48 μm [21]. The spiral in (b) is doped with Er by ion implantation while the spiral in (c) is doped by co-sputtering from a mixed Al_2O_3/Er_2O_3 target. A clear difference is observed: the implanted spiral shows small upconversion, while the co-sputtered spiral shows intense green upconversion (shown in white in the figure). Additional measurements (not shown) showed that the implanted spiral did show net optical gain when pumped at a power of 10 mW ($\lambda = 1.48$ μm) [22], while the co-sputtered one did

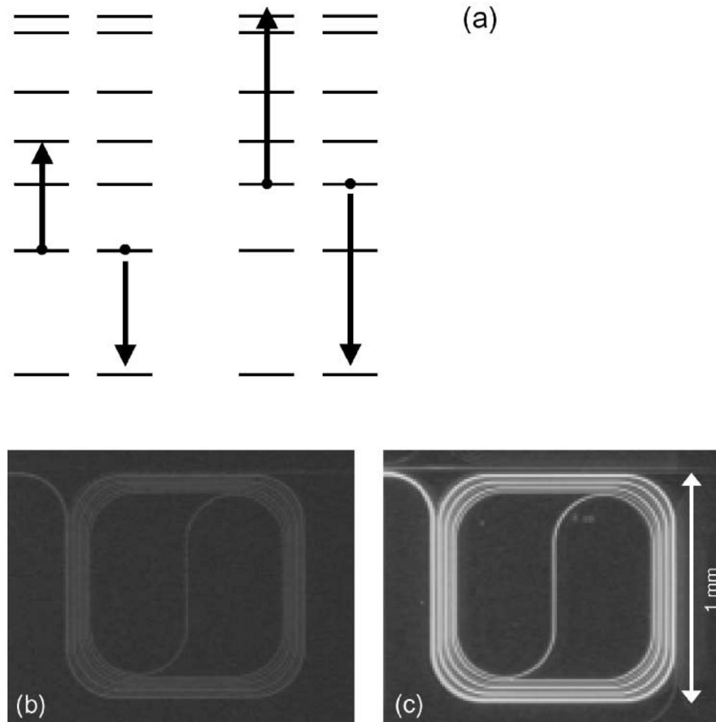

Fig. 5. Erbium as a probe of erbium. (a) Schematic of first- and second-order cooperative upconversion interactions in highly Er-doped materials. Optical images of planar Al_2O_3 waveguide spirals doped with Er by (b) ion implantation or (c) co-sputtering from an Al_2O_3/Er_2O_3 target. The green upconversion luminescence intensity is represented by the white intensity in the images. From Kik et al. [21]. The green emission serves as a probe of the atomic-scale Er distribution in the films.

not. The difference is attributed to the fact that ion implantation leads to a homogeneous atomic-scale distribution of Er, while the co-sputtering process may lead to a strongly inhomogeneous Er distribution, and hence high upconversion. Measurements of the green upconversion emission as shown in Fig. 5 may thus be used as a quick initial probe to investigate if a particular Er-doped waveguide material would be suitable for use in an optical amplifier.

6. Erbium as a probe of radiation damage

Ion implantation is a well-known technique to dope materials with a precisely controlled concentration of impurities at a well-defined depth. During the implantation process, the incident ions lose their energy by causing atomic displacements as well as electronic excitations. Each of these processes leads to the formation of defects. Understanding these irradiation effects in silica glass is important because ion implantation is used for optical doping with Er, as described above. More generally, knowledge of radiation effects in SiO_2 dielectric layers in microelectronic devices or in nuclear waste containers is of great importance.

We have introduced radiation damage into SiO_2 thin films by using a range of different ions at a large ion fluence range. The luminescence lifetime of Er ions pre-implanted into the SiO_2 film was used as a probe of the damage level after irradiation [23]. A 10 μm thick SiO_2 film grown by thermal oxidation was used, and first implanted with 3.5 MeV Er ions to a fluence of $5 \times 10^{15}\,cm^{-2}$. The Er depth profile peaked at 1.25 μm, with a

peak concentration of 0.11 at%. After Er implantation, the film was annealed for 1 h at 900°C in vacuum [24]. Clear photoluminescence from Er was observed after annealing, with a lifetime of 14.1 ms. Subsequently, 1 MeV He, 3.5 MeV C, 5.5 MeV Si or 5.5 MeV Ge ions were implanted in the film at an ion range well beyond the Er depth profile. Fig. 6 shows the luminescence lifetime after irradiation as a function of ion fluence. As can be seen, above an ion fluence of $10^{10}\,cm^{-2}$, the lifetime gradually decreases with fluence. This indicates that the PL lifetime of Er is a sensitive probe of radiation defects as these cause a non-radiative decay channel for the Er ions. The decrease with fluence observed in Fig. 6 is faster for heavier ions, as is expected due to the higher damage generation rate. Quite interestingly, the level at which the lifetime saturates for high fluence is dependent on ion mass: the heavier the ion, the lower the saturation level. Note that the "as-implanted" lifetime of 5.5 ms also fits in the observed trend, as Er is heavier than Ge. The variation in saturation level implies that heavier ions create a "more damaged" saturation state in the glass network. This may be explained in terms of differences in the collision cascade density for light and heavy ions, or differences in the interaction of damage produced by atomic displacements and electronic excitation.

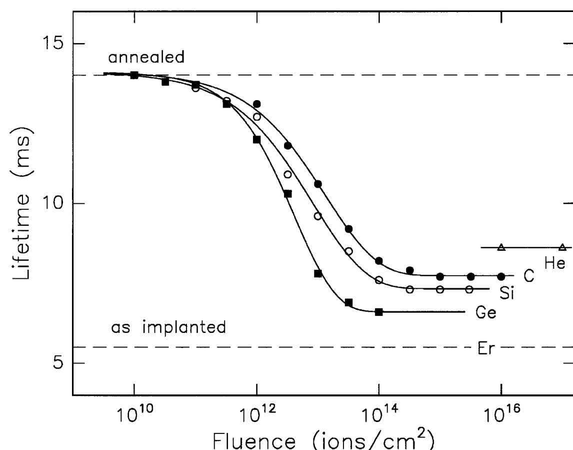

Fig. 6. Erbium as a probe of radiation defects. PL lifetimes of annealed Er-doped SiO_2 films after irradiation with 1 MeV He (triangles), 3.5 MeV C (closed circles), 5.5 MeV Si (open circles) or 8.5 MeV Ge (squares), as a function of fluence. The lifetimes for as-implanted and annealed films are shown by the dashed lines. From Polman and Poate [23]. Radiation defects quench the Er luminescence at a rate depending on ion fluence and mass.

7. Erbium as a probe of glass network structure

The degenerate energy levels of the Er 4f states will split due to the Stark effect when Er is incorporated into a solid host. The shape of the Er luminescence spectrum, which is due to optical transitions between the various Stark levels, hence reflects the local environment around the ion. Indeed, Er PL spectra display quite a variation in shape and width for various materials. The full width at half-maximum for the $^4I_{13/2} \rightarrow {}^4I_{15/2}$ transition around 1.53 μm varies between 11 nm for pure SiO_2 [24] and 70 nm for an Er-doped organic cage complex in solution [18]. In single crystalline hosts, the PL spectrum is usually composed of sharp peaks, while amorphous hosts show more inhomogeneously broadened spectra. We have reported in Ref. [25] a comparison of PL spectra for Er in pure SiO_2 and in sodium silicate glass. It was found that the spectra are quite different: the pure silica shows a broad peak with a single side peak at the high-wavelength side, while the sodium silicate glass shows a split main peak and broad side peaks.

To investigate the difference in local environment around the Er ions in both glasses, EXAFS measurements were performed on the Er L_{III} absorption edge. Fig. 7 shows the Fourier transformed EXAFS data. A bulk Er doped pure SiO_2 sample (Fig. 7(a)) displays two shells: 6 O atoms at 2.28 Å, with a mean square fluctuation of 0.008 $Å^2$ and a second shell composed of Si atoms at a distance of 3.11 Å with a coordination of at least 3. Similar results, but with lower accuracy due to the smaller Er content, were found for Er implanted SiO_2 (Fig. 7(b)). The sodium silica glass (Fig. 7(c)) shows only a first neighbor shell in EXAFS: 6.3 O atoms at a distance of 2.26 Å, with no detectable disorder. No second shell is observed. The difference with the pure silica data is ascribed to the known effect of Na as a network modifier. Na

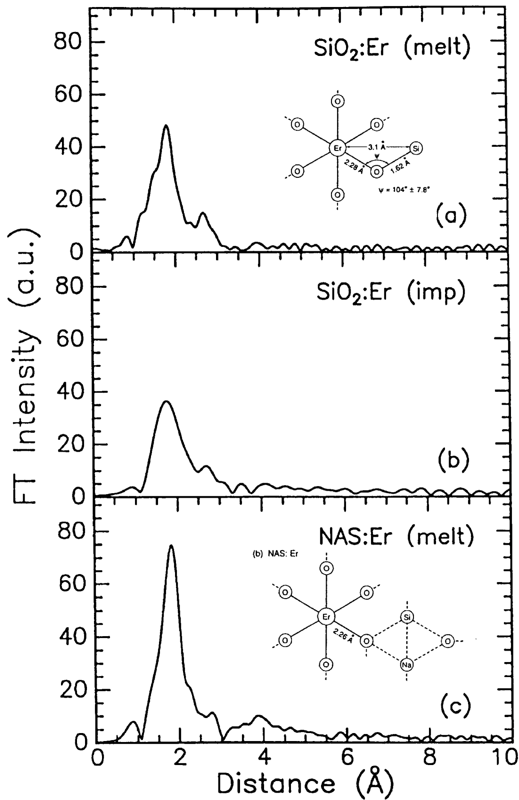

Fig. 7. Erbium as a probe of network structure. Fourier transformed EXAFS data for pure silica doped with Er in the melt (a), silica doped by ion implantation (b) and sodium silicate glass doped in the melt (c). From Marcus et al. [25]. EXAFS spectroscopy on Er inner shells provides a sensitive probe of the silica glass network structure.

may enable the ErO_6 moiety to relax to its lowest energy state, free from the forces applied by the Si–O network. This decoupling results in a narrower Er–O bond length distribution than in pure silica. Since Si, which is part of the network, is now decoupled from the Er, no Er–Si shell is observed. The local configurations around Er derived from the EXAFS data are displayed in the insets in Fig. 7. Using this EXAFS investigation, that employs the inner-shell properties of Er, variations in the network properties of silica glass were determined.

8. Erbium as a probe of excitons

Erbium-doped silicon is an interesting material in which energy transfer can take place between the semiconductor electronic system and the internal 4f states of the rare earth ion. Fig. 8 shows a schematic of the energy bands involved in this system. Si is an indirect bandgap semiconductor with a band gap of 1.123 eV at room temperature. As is common for defects and impurities in semiconductor hosts, an Er impurity in Si provides a trap state, at which electrical carriers can be trapped. In particular, electrons

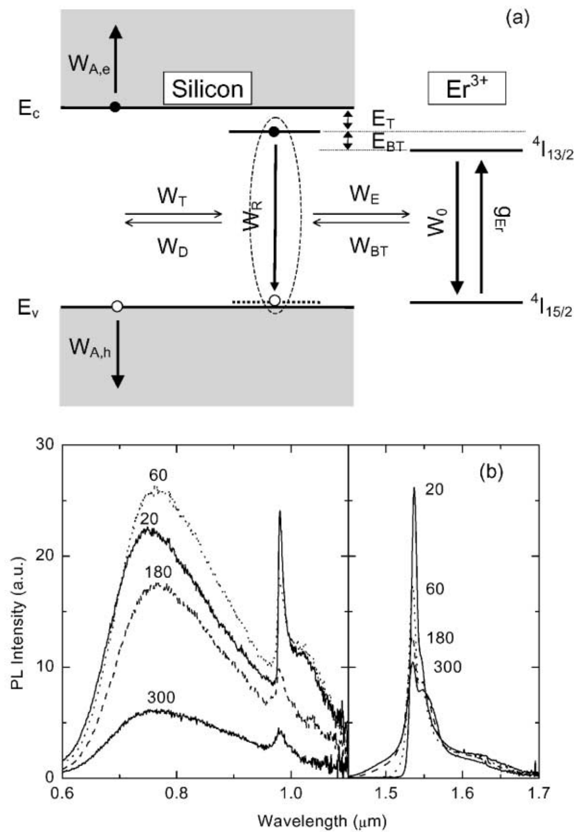

Fig. 8. Erbium as a probe of excitons. (a) Schematic energy level diagram of Er-doped Si. From Hamelin et al. [28]. (b) PL spectra of Er-doped Si nanocrystal/SiO_2 layers, taken at four different temperatures (indicated in K). From Kik et al. [30]. Excitons can be trapped at an Er-related defect in bulk Si or can be quantum confined in a Si nanocrystal; subsequently they can recombine by exciting Er.

and holes may be trapped to form a bound exciton that is spatially located at the position of the Er ion. The case of Er is special, as an Auger energy transfer process can take place in which the bound exciton recombines and the Er ion is excited into the first excited 4f state ($^4I_{13/2}$, 810 meV). The exciton trapping (W_T) and energy transfer (W_E) processes are indicated in Fig. 8(a) by horizontal arrows. Through this mechanism, photoluminescence and electroluminescence from Er in Si have been observed [9,26,27].

Unfortunately, the quantum efficiency of the emission of Er in Si is small (10^{-4}) at room temperature. From temperature dependent measurements we have found [28] that a main quenching mechanism is a backtransfer process (W_{BT} in Fig. 8(a)) in which excited Er is not de-excited radiatively but by the generation of a bound exciton. This exciton can then dissociate leading to the formation of free carriers (W_D in Fig. 8(a)). While this process seems unlikely due to the large mismatch (300 meV) between the first excited state of Er and the Si bandgap, in fact it is not: the internal backtransfer efficiency is 70% at room temperature. This is due to the fact that the radiative lifetime of Er is very long (1 ms). As a result, the 300 meV barrier (that is taken in two steps, see Fig. 8(a)) can be taken at high efficiency. See Ref. [28] for a more detailed description of these processes.

One way to reduce the backtransfer process is by increasing the bandgap of Si. This can be done by using silicon quantum dots in which the exciton energy increases with decreasing size, due to a quantum confinement effect [29]. We have fabricated SiO_2 films doped with a high concentration of Si quantum dots, co-doped with Er. It was found that the Er can be very efficiently optically excited through the recombination of quantum confined excitons that are optically generated in the nanocrystals [30–33]. Fig. 8(b) shows PL spectra of Er and Si nanocrystal (3–5 nm diameter) doped SiO_2, taken at different temperatures. No thermal quenching of the integrated Er emission intensity is observed, which is ascribed to the large bandgap mismatch between the first excited state of Er and Si nanocrystals. In this nanocrystal/Er material, the Si nanocrystals act as "sensitizer" for Er. As the nanocrystal absorption spectrum is broad, with an absorption cross section that is 4–6 orders of magnitude higher than that of the Er 4f levels, this holds great promise for the use of this material in optical amplifiers as the (expensive) pump laser that is used in such devices may now be replaced by a broad band light source.

9. Erbium as a probe of local optical density of states

The spontaneous emission of an atom is not a property of the atom only, but depends on the local optical surrounding as well. The simplest demonstration of this effect was shown for a luminescent ion close to a mirror or a dielectric interface [34–36]. In this case, the emission rate depends on the position of the atom relative to the reflecting boundary. The changes in decay rate can be determined by calculating the local optical density of states (DOS) and then applying Fermi's Golden Rule to obtain the radiative rate. It has been shown that the radiative rate is proportional to the DOS, both in scalar approximation and for the full Maxwell equations. Recently, there has been growing interest in the use of more complicated dielectric structures such as microcavities and photonic crystals to modify the rate of spontaneous emission.

Fig. 9(a) shows calculations of the local optical density of states for a three-dimensional spherical microcavity with a refractive index of 1.45 (e.g. SiO_2) at a vacuum wavelength of 1.536 μm [37]. The DOS is calculated as a function of diameter (horizontal axis) and normalized radial distance (vertical axis), and is indicated by a gray scale normalized to the DOS in bulk SiO_2. Several minima and maxima in the DOS are observed as a function of cavity diameter, and can be related to Mie resonances or normal modes of the microcavity. The positions of these modes are indicated on the top axis. The magnetic (electric) resonances are labeled $M_n^l(E_n^l)$, where n corresponds to the order of the resonance, $l = 1$ corresponds to the ground tone of a resonance, while higher l indicates overtones.

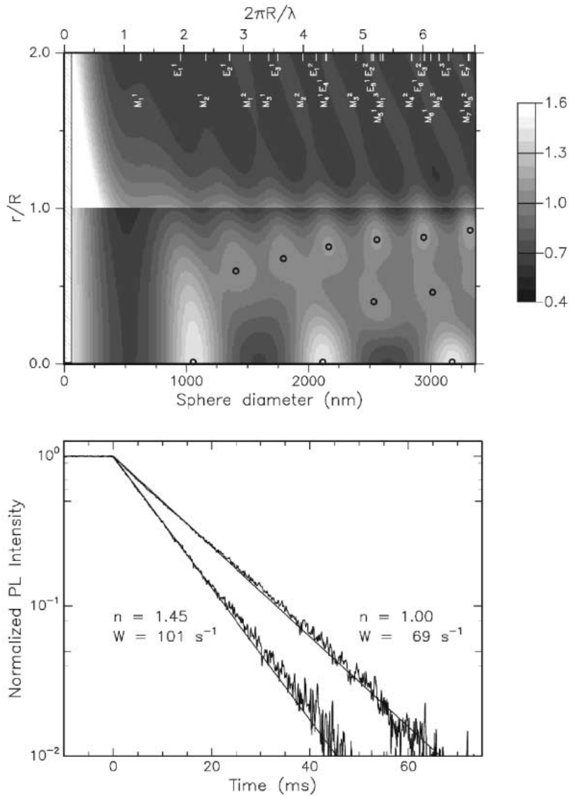

Fig. 9. Erbium as a probe of optical density of states. (a) Calculated DOS in a spherical SiO_2 microcavity as a function of diameter (horizontal axis) and normalized radial distance (vertical axis). The DOS is indicated by a gray scale (see bar on the right-hand side), with DOS = 1.0 corresponding to the DOS in bulk SiO_2. (b) PL decay measurements at 1.535 μm of Er-doped SiO_2 microcavities in air and in an index-matching fluid ($n = 1.45$). From de Dood et al. [37]. The variation in DOS by modifying the optical surrounding of the microcavities is probed using measurements of the Er decay time.

To experimentally probe the local DOS, Er ions were implanted in 340 nm diameter SiO_2 microspheres fabricated by using the Stöber reaction [38]. Fig. 9(b) shows PL decay measurements for Er-implanted spheres in air: the decay time is 14.5 ms. The implanted spheres were then immersed in an index-matching fluid ($n = 1.45$, see Fig. 9(b)) and the PL decay was measured again: 9.9 ms. This difference is attributed to changes in the local DOS that occur due to the index matching [35,39]. More details on the analysis, as well as the separation of both radiative and non-radiative decay components in Er that is possible using these experiments, are described in Ref. [37].

10. Erbium as a probe of optical modes

The design of integrated optical circuits depends heavily on the modeling of the propagation of optical modes. In the past 10 years, great progress has been made in the development of modeling tools. At the same time, experimental methods to determine the distribution and propagation of optical modes in planar waveguides have remained scarce. This has made it difficult to compare calculated mode profiles with experimental ones. One method that is being used is to detect with an optical microscope the distribution of light that is scattered from the waveguide. This method is unreliable since the distribution of scatter centers in the waveguide is often unknown. Moreover, its resolution is limited by the diffraction limit. Near-field optical probes could be used to overcome this problem, but at the same time, are known to affect the propagation of the modes themselves.

We have developed a novel technique by which optical mode distributions can be imaged with great precision, at a resolution below the diffraction limit [40]. We employ the use of Er ions incorporated in the waveguide that are pumped into the first excited state using a 1.48 μm laser. The Er concentration chosen is so high (1.4 at%) that cooperative upconversion (see Section 5) takes place, leading to significant population of higher lying states. The spontaneous emission from these states is then imaged using optical microscopy. Fig. 10(a) shows an image of the intensity of green light (540 nm, $^4S_{3/2} \rightarrow {}^4I_{15/2}$ transition) emitted from a planar multi-mode interference coupler made in Al_2O_3. In this device, light is coupled-in through a single-mode waveguide at the left-hand entrance. In the multi-mode section, starting at distance = 0 in the figure, a multi-mode interference pattern builds up, that can be used to cause an even splitting of the light intensity at specific locations along the length of the waveguide (indicated by arrows labeled 2–4 in the figure). The green image provides an accurate determination of the 1.48 μm-pump distribution in

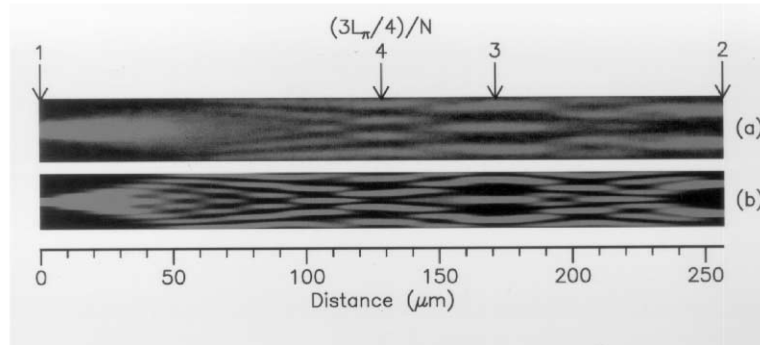

Fig. 10. Erbium as a probe of optical modes. (a) Optical microscopy image of an Er-doped multi-mode interference coupler pumped at 1.48 μm. The green upconversion emission is represented by the white intensity in the figure. (b) Calculated emission pattern. From van den Hoven et al. [40]. Imaging of the Er upconversion emission can be used to probe the propagation of optical modes in complicated photonic structures.

the waveguide. Fig. 10(b) shows the calculated upconversion emission profile, it clearly resembles the measured data. An image of the red emission (660 nm, $^4F_{9/2} \rightarrow {}^4I_{15/2}$ transition) was also taken, and showed exactly the same pattern as shown in Fig. 10. In this technique the detection wavelength is much smaller than the wavelength of the imaged modes, and thus the resolution can be smaller than the diffraction limit. This imaging technique can be used to verify if fabricated structures operate as modeled, and to study more complicated waveguide designs where modeling is inaccurate.

11. Erbium as a probe of optical bandstructure

A photonic crystal is defined as a regularly arranged dielectric structure in which a strong interaction with light takes place. An example of a photonic crystal in one dimension is a multilayer of materials with alternating refractive index which can act as a Bragg reflector or Fabry–Perot cavity, in which the reflection and transmission of light is a strong function of wavelength. In two dimensions, a photonic crystal can be composed of, e.g. regularly arranged holes in a dielectric slab or a regularly structured array of dielectric cylinders. In three dimensions, a variety of periodic structures have been made using lithographic techniques or self-assembly methods using colloidal techniques. The general challenge in photonic crystal research is to design crystals such that their optical band structure shows a gap, i.e. a band of frequencies that is not allowed in the crystal for one or two polarizations.

Once these structures are made, it is a challenge to actually probe their optical properties. Fig. 11 shows a two-dimensional photonic crystal based on Si pillars made by using electron cyclotron resonance etching techniques [41]. The Si pillars, arranged on a cubic lattice, are 5 μm tall, spaced by 550 and 240 nm in diameter. Band structure calculations indicate the presence of a broad gap [39], which for the geometry in Fig. 11(a) is centered on a wavelength of 1.53 μm. Note that silicon is transparent at this wavelength. Indeed, due to the high level of precision available in Si processing, Si is an ideal base material to fabricate photonic crystals. To experimentally probe the optical bandstructure of the photonic crystals in Fig. 11(a), waveguides are integrated so that light can be coupled in and out. In order to confine light in the third dimension, the top section of the Si pillars is turned amorphous by Xe ion irradiation (a-Si has a higher refractive index than crystalline Si) [39]. Measurements on these structures are underway.

An alternative method to probe the optical bandstructure is to incorporate optical probe ions in the crystal, and to measure the spontaneous emission rate and polarization dependence of the emission. We have developed a wet-chemical

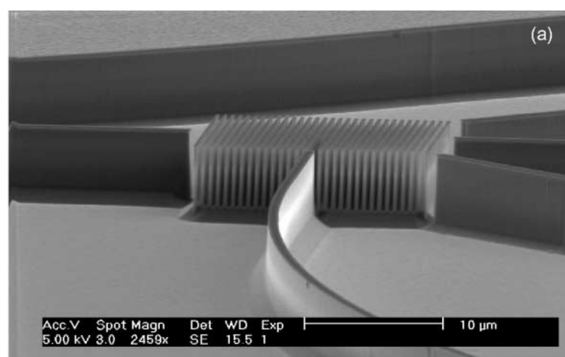

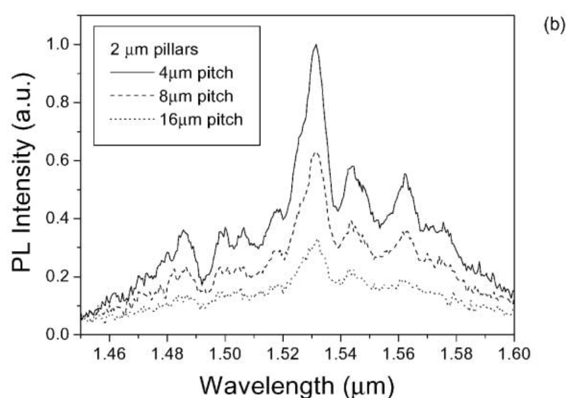

Fig. 11. Erbium as a probe of photonic bandstructure. (a) Two-dimensional Si photonic crystal composed of 5 μm tall Si pillars on a cubic lattice. In- and output waveguides are integrated with the photonic crystal from Zijlstra et al. [41]. (b) PL spectrum of a Si photonic crystal coated with Er using a wet-chemical technique ($\lambda_{pump} = 488$ nm). Data are shown for a pitch of 4, 8, and 16 μm. From Isshiki et al. [42]. The spontaneous emission from Er can be used to probe the photonic bandstructure of photonic crystals.

process to coat a Si photonic crystal with optically active Er ions [42]. The sample is dipped in an $ErCl_3$ solution and subsequently oxidized and annealed. Fig. 11(b) shows the PL spectra of pillar structures with relatively large pitch (4, 8, and 16 μm). The PL intensity increases for decreasing pitch, due to the larger surface area excited in the laser spot. The next challenge is to measure the effect of the photonic bandstructure on the Er emission at 1.53 μm from structures with smaller pitch that have a bandgap centered around 1.5 μm.

12. Conclusions

Erbium ions can be used to probe point defects, oxygen, OH, Er, radiation defects, network structure, excitons, optical density of states, optical modes, and photonic bandstructure. The future will learn what other probing effects of erbium may be discovered.

Acknowledgements

This paper is written to celebrate the 10th anniversary of the Opto-electronic materials group at AMOLF, founded in 1991. It is the result of the hard work and creative ideas of all (previous) group members including *Ph.D. students*: Edwin Snoeks, Gerlas van den Hoven, Mark Brongersma, Pieter Kik, Lenneke Slooff, Christof Strohhöfer, Michiel de Dood, Teun van Dillen, and Jeroen Kalkman; *post-docs and guests:* Jon Custer, Salvo Coffa, Jung Shin, Rosalia Serna, Kostya Kikoin, Mariëlle Ladevèze, Tadamasa Kimura, José dos Santos, Nicholas Hamelin, and Hideo Isshiki; *advisors*: Frans Saris and Jan van der Elsken; *undergraduate students*: Erik Radius, Daniel Peters, Freek Suyver, Dirk Vossen, Michael Hensen, Basjan Berkhout, and Joan Penninkhof; *technical support*: Simon Doorn, Johan Derks and Jan ter Beek. I gratefully acknowledge the fruitful previous and ongoing collaborations with Dale Jacobson, Mathew Marcus and John Poate (Bell Labs, NJ), Salvo Coffa, Salvo Lombardo, Giorgia Franzò, Francesco Priolo and the late Ugo Campisano (CNR-IMETEM, Catania), Martin Fleuster and Chris Buchal (Research Center Jülich), Kyu Min and Harry Atwater (CALTECH, Pasadena, CA), Eduardo Alves and José Soares (Lisbon), Franco Cacciali and Richard Friend (Cambridge University), Ben Hendriksen and Mart Diemeer (KPN Research), Cor van Dam, Koos van Uffelen and Meint Smit (Technical University Delft), Tony Zijlstra and Emile van der Dift (DIMES, Delft), Ad Lagendijk (University of Amsterdam), Manon Oude Wolbers, Steve Klink, Gerald Hebbink, and Frank van Veggel (Twente University), Hans Hofstraat (Philips Research), Anne-Jans Faber and Yingchao Yan

(TNO-TPD), Alexander Moroz and Alfons van Blaaderen (AMOLF, Utrecht University) and Adriaan Tip (AMOLF).

This work is part of the research program of the Foundation for Fundamental research on Matter (FOM) and is financially supported by the Dutch Organization for Scientific Research (NWO). Separate sections of this work were funded by the Dutch Technology Foundation (STW), the Innovative research program IOP-Electro-optics of the Ministry of Economic Affairs, and the Esprit program of the European Union.

References

[1] T. Förster, E. Koning, Z. Elektrochem. 61 (1957) 344.
[2] G. Blasse, B.C. Grabmeier, Luminescent Materials, Springer Verlag, Berlin, 1994.
[3] S. Roorda, W.C. Sinke, J.M. Poate, D.C. Jacobson, S. Dierker, B.S. Dennis, D.J. Eaglesham, F. Spaepen, P. Fuoss, Phys. Rev. B 44 (1991) 3702 and references therein.
[4] A. Polman, J.S. Custer, E. Snoeks, G.N. van den Hoven, Appl. Phys. Lett. 62 (1993) 507.
[5] A. Polman, J.S. Custer, P.M. Zagwijn, A.M. Molenbroek, P.F.A. Alkemade, J. Appl. Phys. 81 (1997) 150.
[6] J.S. Custer, A. Polman, M.H. van Pinxteren, J. Appl. Phys. 75 (1994) 2809.
[7] P.N. Favennec, H. lHaridon, D. Moutonnet, M. Salvi, M. Gauneau, J. Appl. Phys. 29 (1990) L524.
[8] J. Michel, J.L. Benton, R.F. Ferrante, D.C. Jacobson, D.J. Eaglesham, E.A. Fitzgerald, Y.-H. Xie, J.M. Poate, L.C. Kimerling, J. Appl. Phys. 70 (1991) 2672.
[9] S. Coffa, G. Franzò, F. Priolo, A. Polman, R. Serna, Phys. Rev. B 49 (1994) 16313.
[10] D.L. Adler, D.C. Jacobson, D.J. Eaglesham, M.A. Marcus, J.L. Benton, J.M. Poate, P.H. Citrin, Appl. Phys. Lett. 61 (1992) 2181.
[11] S. Coffa, F. Priolo, G. Franzó, V. Bellani, A. Carnera, C. Spinella, Mat. Res. Soc. Symp. Proc. 301 (1993) 125.
[12] R. Serna, M. Lohmeier, P.M. Zagwijn, E. Vlieg, A. Polman, Appl. Phys. Lett. 66 (1995) 1385.
[13] J.F. Suyver, P.G. Kik, T. Kimura, A. Polman, G. Franzò, S. Coffa, Nucl. Instr. and Methods B 148 (1999) 497.
[14] P.G. Kik, A. Polman, MRS Bull. 23 (1998) 48.
[15] E. Snoeks, G.N. van den Hoven, A. Polman, J. Appl. Phys. 73 (1993) 8179.
[16] E. Snoeks, P.G. Kik, A. Polman, Opt. Mater. 5 (1996) 159.
[17] V.P. Gapontsev, A.A. Izyneev, Yu.E. Sverchov, M.R. Syrtlanov, Sov. J. Quantum Electron 11 (1981) 1101.
[18] L.H. Slooff, A. Polman, M.P. Oude Wolbers, F.C.J.M. van Veggel, D. Reinhoudt, J.W. Hofstraat, J. Appl. Phys. 83 (1998) 497.
[19] E. Snoeks, G.N. van den Hoven, A. Polman, B. Hendriksen, M.B.J. Diemeer, F. Priolo, J. Opt. Soc. Am. B12 (1995) 1468.
[20] G.N. van den Hoven, E. Snoeks, A. Polman, C. van Dam, J.W.M. van Uffelen, M.K. Smit, J. Appl. Phys. 79 (1996) 1258.
[21] P.G. Kik, A. Polman, J.W.M. van Uffelen, M.K. Smit, in preparation.
[22] G.N. van den Hoven, E. Snoeks, A. Polman, J.W.M. van Uffelen, Y.S. Oei, M.K. Smit, Appl. Phys. Lett. 62 (1993) 3065.
[23] A. Polman, J.M. Poate, J. Appl. Phys. 73 (1993) 1669.
[24] A. Polman, D.C. Jacobson, D.J. Eaglesham, R.C. Kistler, J.M. Poate, J. Appl. Phys. 70 (1991) 3778.
[25] M.A. Marcus, A. Polman, J. Non-Cryst. Solids 136 (1991) 260.
[26] G. Franzò, F. Priolo, S. Coffa, A. Polman, A. Carnera, Appl. Phys. Lett. 64 (1994) 2235.
[27] B. Zheng, J. Michel, F.Y.G. Ren, L.C. Kimerling, D.C. Jacobson, J.M. Poate, Appl. Phys. Lett. 64 (1994) 2842.
[28] N. Hamelin, P.G. Kik, J.F. Suyver, K. Kikoin, A. Polman, A. Schönecker, F.W. Saris, J. Appl. Phys. 88 (2000) 5381.
[29] M.L. Brongersma, P.G. Kik, A. Polman, K.S. Min, H.A. Atwater, Appl. Phys. Lett. 76 (2000) 351.
[30] P.G. Kik, M.L. Brongersma, A. Polman, Appl. Phys. Lett. 76 (2000) 2325.
[31] P.G. Kik, A. Polman, J. Appl. Phys. 88 (2000) 1992.
[32] M. Fujii, M. Yoshida, Y. Kanzawa, S. Hayashi, K. Yamamoto, Appl. Phys. Lett. 71 (1997) 1198.
[33] G. Franzò, V. Vinciguerra, F. Priolo, Appl. Phys. A. 69 (1999) 3.
[34] K.H. Drexhage, J. Lumin. 12 (1970) 693.
[35] E. Snoeks, A. Lagendijk, A. Polman, Phys. Rev. Lett. 74 (1995) 2459.
[36] T.M. Hensen, M.J.A. de Dood, A. Polman, J. Appl. Phys. 88 (2000) 5142.
[37] M.J.A. de Dood, L.H. Slooff, A. Moroz, A. van Blaaderen, A. Polman, Phys. Rev. A, in press (2001).
[38] A. van Blaaderen, A. Vrij, Langmuir 8 (1993) 2921.
[39] M.J.A. de Dood, E. Snoeks, A. Moroz, A. Polman, IEE Opt. Quant. Elec. (2001), in press.
[40] G.N. van den Hoven, A. Polman, C. van Dam, J.W.M. van Uffelen, M.K. Smit, Opt. Lett. 21 (1996) 576.
[41] T. Zijlstra, E.W.J.M. van der Drift, M.J.A. de Dood, E. Snoeks, A. Polman, J. Vac. Sci. Technol. B17 (1999) 2734.
[42] H. Isshiki, M.J.A. de Dood, T. Kimura, A. Polman, in preparation.